

Article

Lithium-Doped Biological-Derived Hydroxyapatite Coatings Sustain In Vitro Differentiation of Human Primary Mesenchymal Stem Cells to Osteoblasts

Paula E. Florian ^{1,*} , Liviu Duta ^{2,*} , Valentina Grumezescu ², Gianina Popescu-Pelin ², Andrei C. Popescu ³, Faik N. Oktar ^{4,5}, Robert W. Evans ⁶ and Anca Roseanu Constantinescu ¹

¹ Institute of Biochemistry, Romanian Academy, 060031 Bucharest, Romania; roseanua@gmail.com

² National Institute for Lasers, Plasma and Radiation Physics, 077125 Magurele, Romania; valentina.grumezescu@inflpr.ro (V.G.); gianina.popescu@inflpr.ro (G.P.-P.)

³ Center for Advanced Laser Technologies (CETAL), National Institute for Lasers, Plasma and Radiation Physics, 077125 Magurele, Romania; andrei.popescu@inflpr.ro

⁴ Department of Bioengineering, Faculty of Engineering, Marmara University, Goztepe Campus, 34722 Istanbul, Turkey; foktar@marmara.edu.tr

⁵ Center of Nanotechnology & Biomaterials Application & Research, Marmara University, Goztepe Campus, 34722 Istanbul, Turkey

⁶ School of Engineering and Design, Brunel University, London UB8 3PH, UK; robertwevans49@gmail.com

* Correspondence: florian_paula@yahoo.com (P.E.F.); liviu.duta@inflpr.ro (L.D.); Tel.: +40-214574558 (L.D.)

Received: 27 October 2019; Accepted: 18 November 2019; Published: 21 November 2019



Abstract: This study is focused on the adhesion and differentiation of the human primary mesenchymal stem cells (hMSC) to osteoblasts lineage on biological-derived hydroxyapatite (BHA) and lithium-doped BHA (BHA:LiP) coatings synthesized by Pulsed Laser Deposition. An optimum adhesion of the cells on the surface of BHA:LiP coatings compared to control (uncoated Ti) was demonstrated using immunofluorescence labelling of actin and vinculin, two proteins involved in the initiation of the cell adhesion process. BHA:LiP coatings were also found to favor the differentiation of the hMSC towards an osteoblastic phenotype in the presence of osteoinductive medium, as revealed by the evaluation of osteoblast-specific markers, osteocalcin and alkaline phosphatase. Numerous nodules of mineralization secreted from osteoblast cells grown on the surface of BHA:LiP coatings and a 3D network-like organization of cells interconnected into the extracellular matrix were evidenced. These findings highlight the good biocompatibility of the BHA coatings and demonstrate that the use of lithium as a doping agent results in an enhanced osteointegration potential of the synthesized biomaterials, which might therefore represent viable candidates for future in vivo applications.

Keywords: biological-derived hydroxyapatite coatings; lithium doping; pulsed laser deposition; human mesenchymal stem cells; osteoblasts

1. Introduction

Surface properties of the biomaterials used for implants, such as chemistry and topography, are of crucial importance in establishing the tissue response to the success or failure of an implant [1–4]. Titanium (Ti) implants have been widely used in dental and orthopedic fields for bone replacement and tissue engineering due to their remarkable performances [5,6]. Current Ti surface functionalization focuses on simple and doped hydroxyapatite (HA) coatings as bioactive alternatives to autogenous bone for osseous remodeling processes [7–9].

Synthetic hydroxyapatite (HA) is a well-known biocompatible material used as an implantable ceramic for bone replacement due to its chemical-structural similarity with the inorganic part of

human bone tissues [10]. It is stable in simulated biological fluids and exhibits an osteoconductive behavior [11,12]. Despite this capacity, HA ceramics possess weak mechanical properties [13]. To overpass this drawback, synthetic HA can be applied as a thin coating onto the surface of metallic implants, aiming to improve fixation at the living tissue—implant interface and to determine bone regeneration/formation [14].

It is worth noting that a great challenge in the biomedical field is the development of implants which could be easily integrated into the living body [15–17]. Biological-derived hydroxyapatite (BHA), which demonstrated exhibiting excellent biocompatibility, bioactivity, and osseointegration characteristics [18], can serve as an alternative to conventional synthetic HA. Moreover, BHA materials doped with specific elements such as Ti, Li_2CO_3 , Li_2O , Li_3PO_4 , MgF_2 , and/or MgO were reported to be a viable solution to improve the mechanical characteristics and to enhance the biological efficiency of an implant, due to their close resemblance with bone apatite [19]. One should stress upon the fact that the Earth's available mineral resources are threatened to become limited in the near future because of the rapid demographic increase and economic growth. Therefore, the access to low-cost sustainable natural resources (i.e., HA derived from animal bones, like in the current study) is critical, and consequently highly encouraged, for future economic growth and human welfare. The possibility to independently vary a large number of parameters (i.e., the laser fluence, pulse repetition rate, energy, target-to-substrate separation distance, substrate temperature, nature and pressure of the gas in the deposition chamber), on one hand, and the safety in functioning, fast processing, and low production costs, on the other hand, have advanced PLD, in the field of thin film growth, as a simple and versatile technique to produce layers with a high diversity of morphological and structural characteristics, which are superior to the ones pertaining to conventional deposition techniques [20–22]. For the difference of synthetic HA, natural apatites contain trace elements and new functional groups (i.e., HPO_4^{2-} and CO_3^{2-}) in their complex molecules. In this respect, the transfer of animal-origin HA by PLD is highly attractive due to the main advantage of this technique to grow stoichiometric films, with a controlled degree of crystallinity and thickness. One should note that these characteristics have a key influence over bio-resorption or dissolution, which are directly implicated in the process of films' osseointegration.

In our previous study [23], BHA:LiP coatings were shown both to exhibit a hydrophilic behavior as compared to bare Ti (control) and simple BHA coatings and to promote the human mesenchymal stem cells (hMSC) growth on the film surface, while maintaining an excellent adherence to the metallic substrate and evidencing a long-lasting anti-staphylococcal and -fungal biofilm activity [24]. The differentiation of hMSC to osteoblasts (OB) is a well-known model for bone regeneration used in the study of biocompatibility of materials proposed for implants [25,26].

Based on these observations, a leap forward in our research was performed by investigating the capacity of lithium-doped BHA (further denoted as BHA:LiP) coatings to promote the *in vitro* differentiation of primary hMSC from bone marrow aspirates to OB lineage. The expression of cell adhesion, cell morphology and OB specific markers were analyzed by fluorescence and Scanning Electron microscopy (SEM). Alkaline phosphatase (ALP) activity, an early key marker of osteogenesis, was quantitatively assessed to evaluate the capacity of BHA:LiP coatings to support the differentiation of hMSC to OB phenotype. To the best of our knowledge, this is the first evidence that synthesized BHA:LiP layers could offer proper conditions for hMSC adhesion and OB differentiation and sustain the achievement of an enhanced osseointegration potential for a new generation of metallic implants.

2. Materials and Methods

2.1. Powders Preparation

BHA powders were obtained from the cortical part of bovine femoral bones, following the protocol previously described in [20]. Briefly, the heads of femoral bones were cut off and the shafts processed. The bone marrows were then extracted and the soft tissue residues gently removed from

the shafts. The femoral shafts were further cut into slices, cleaned and washed with distilled water and deproteinized for 14 days in an alkali media of 1% sodium hypochlorite. The resulting dry bone fragments were submitted to a calcination process (at 850 °C, 4 h in air), to remove any residual organic or biological hazardous components [27,28]. Before undergoing ball-milling to fine powders, the calcined bone specimens were crushed with a mortar and pestle. It should be emphasized that, for the fabrication of BHA powders, European Regulations [29] and ISO standard [30] were followed.

Batches of BHA powders were admixed with 1 wt.% of Li_3PO_4 (Sigma-Aldrich GmbH, St. Louis, MO, USA) and used for comparison.

2.2. Target Preparation

BHA and BHA:LiP powders were pressed at ~5 MPa in a 20 mm diameter mold. The resulting pellets were thermally treated in air, using an oven, for 4 h, at 700 °C. A heating rate of 20 °C/min and a cooling ramp of 5 °C/min were applied. Following this protocol, the fabrication of hard and compact targets, which are suited for PLD experiments, was achieved.

2.3. PLD Experiment

The PLD experiments were performed inside of a stainless-steel deposition chamber, in a pressure of 50 Pa water vapors. A KrF* excimer laser source, model COMPexPro 205 from Lambda Physics-Coherent, Göttingen, Germany ($\lambda = 248$ nm, $\tau_{\text{FWHM}} \leq 25$ ns), running at a repetition rate of 10 Hz, was used for the target ablation. The laser fluence was set at ~3.5 J/cm² (with a corresponding laser pulse energy of ~360 mJ). The laser beam was incident at 45° on the target surface. The ablated material was collected onto Ti substrates, with dimensions of (0.7 × 0.7) cm², which were placed parallel to the targets, at a separation distance of 5 cm. During the multi-pulse laser irradiation, the target was continuously rotated with 0.3 Hz and translated along two orthogonal axes to avoid piercing and to obtain unidirectional plasma. In addition, the substrates were heated and maintained at a constant temperature of 500 °C using a PID-EXCEL temperature controller (EXCEL Instruments, Mumbai, India), with a heating rate of 25 °C/min and a cooling ramp of 10 °C/min. Keeping the same parameters intact for the growth of one film, 15,000 consecutive laser pulses were applied.

Prior to introduction into the deposition chamber, the substrates were successively cleaned following a three-step protocol, implemented in our laboratory: acetone, ethylic alcohol, and deionized water, for 15 min each. Furthermore, to avoid any possible micro-contamination, the targets were submitted to a “cleaning” process with ~2000 laser pulses. To collect the flux of expelled micro-impurities, a shutter was interposed between the target and the substrate.

To improve the crystallinity of the synthesized coatings, all samples were submitted to a 6 h post-deposition thermal treatment in water vapors enriched atmosphere, at a temperature of 600 °C.

2.4. Cell Culture

Primary hMSC were obtained from bone marrow aspirates and isolated by density gradient centrifugation, as previously described in Ref. [31]. Bone marrow was harvested from one healthy patient undergoing surgery for the orthopaedic implant procedure, with the approval of the Ethics Committee of the University of Medicine and Pharmacy of Craiova (Reference No. 68/11 July 2016). Human primary OB cells were obtained by differentiation of the hMSC.

The hMSC at low passage (2) were grown in complete Dulbecco's Modified Eagle Medium (DMEM) with low glucose (1 g/L), supplemented with 10% (*v/v*) fetal bovine serum (FBS) and 1% (*v/v*) streptomycin/penicillin (all from Gibco (Life Technologies, Paisley, UK)). For *in vitro* OB differentiation, the hMSC were grown in complete Minimum Essential Medium Alpha (α -MEM—Gibco, Thermo Fisher Scientific (Life Technologies, Paisley, UK)), supplemented with osteogenic factors: 82 $\mu\text{g/mL}$ ascorbic acid (Sigma, Saint Louis, MO, USA), 100 nM dexamethasone (Sigma) and 10 mM β -glycerophosphate (Santa Cruz Biotechnology, (Dallas, Texas, USA)) [32]. The cells were maintained in culture at a density of 5×10^3 cells/cm² in 24-well plates, for 1, 3, and 21 days, respectively.

2.4.1. Cell Adhesion and Differentiation

Osteogenic Differentiation

The hMSC were cultivated in complete α -MEM or in complete α -MEM supplemented with osteogenic factors (osteoinduction medium, OIM), if differentiation to osteogenic phenotype was envisaged. Both hMSC and OB were cultivated in 24-well plates on the surface of Ti, BHA, and BHA:LiP coatings. All materials used for biocompatibility investigations were sterilized in a *Falcon 30 Autoclave* (LTE Scientific, (Greenfield, Oldham, UK)) using water vapors at 121 °C and 1 atm, for 30 min, before interaction with the cells. The cell adhesion and specific differentiation markers were assessed by immunofluorescence techniques.

The cells were cultivated for one and three days, then fixed with 4% paraformaldehyde (PFA) for 10 min and permeabilized with 0.2% Triton X-100 solution. Unspecific sites were blocked for 1 h with 0.5% bovine serum albumin solution. Cells were labeled with primary mouse anti-human vinculin antibodies (Sigma-Aldrich, Saint Louis, MO, USA) for 30 min before incubation with secondary antibodies goat anti-mouse conjugated with *Alexa Fluor 594* (Thermo Fisher Scientific, CA, USA). For actin filaments labeling, the samples were incubated for 30 min with phalloidin reagent conjugated with *Alexa Fluor 488* (Thermo Fisher Scientific). The nuclei were counterstained with Hoechst fluorescent dye (Life Technologies, Molecular Probes, Eugene, OR, USA). After the incubation period, the samples were mounted for microscopy investigation with *Medium Prolong Gold AntiFade* (Life Technologies). Samples were visualized using a *Zeiss AxioCam Erc5s* fluorescence microscope with *ApoTome 2* module and image acquisition was performed using *AxioCam MRm* camera (20 \times and 40 \times objectives). For image editing, the *Axio Vision Rel 4.8* software was utilized (Zeiss, Jena, Germany).

The differentiation capacity of the hMSC towards osteogenic phenotype was investigated using specific markers, such as osteocalcin and ALP.

ALP Activity Assay

The detection and quantification of ALP were performed using a colorimetric enzymatic assay (Quantitative Alkaline Phosphatase ES Characterization Kit, CHEMICON, Millipore (Darmstadt, Germany)). Briefly, the hMSC and OB were grown onto the surface of Ti, BHA, and BHA:LiP coatings for 14 days. The cell supernatant was then removed and the samples covered with cells were moved in a new 24-well plate for ALP activity measurements. After successive washing steps, using phosphate saline buffer, the cells were incubated with p-nitrophenyl phosphate substrate buffer to initiate the enzymatic hydrolysis. The absorbance level of yellow-colored by-product p-nitrophenol produced in the reaction was read at 405 nm in a spectrophotometer (Mithras, Berthold Technologies, Bad Wildbad, Germany) and was proportional with the amount of ALP present within the reaction. The ALP present in the sample was quantified using a standard curve of recombinant ALP present in the kit. All experiments were performed in triplicate.

Osteocalcin Detection

For osteocalcin protein detection in hMSC and OB grown on the surface of Ti, BHA and BHA:LiP coatings, a protocol for immunofluorescence—similar to the one for actin/vinculin detection described above—was applied. Briefly, the cells were cultivated for 1 and 21 days, then fixed and permeabilized before incubation with rabbit polyclonal primary anti-human osteocalcin antibodies (CHEMICON, Millipore). The detection was performed using a secondary antibody goat anti-rabbit conjugated with *Alexa Fluor 594* (Molecular Probes, Eugene, OR, USA).

2.4.2. Mineralization Assay

The extracellular matrix mineralization by OB was demonstrated by Alizarin Red staining [33,34]. Briefly, the cells were fixed with 4% PFA, and stained with a solution of 40 mM, pH 4.1 Alizarin Red S, for 30 min. Excess stain was removed with several distilled water washing steps. Finally, the cells

were air-dried and the deposited Alizarin Red S dye was dissolved in a solution with 10% acetic acid and 20% methanol for 30 min. The absorbance of the resulting solution was recorded at a wavelength of 450 nm using a Berthold microplate reader (Bad Wildbad, Germany), whilst the quantification was performed using a standard curve of the dye.

2.4.3. SEM

To investigate the discrete features of cellular morphology in the presence of biomaterials, the hMSC and OB grown onto the surfaces of Ti, BHA, and BHA:LiP coatings for 14 and 21 days were prepared for SEM imaging. Briefly, the cells were fixed with 2.5% glutaraldehyde solution and then dehydrated by sequential immersion in 70%, 90% and 100% ethanol. All specimens were washed with 50% and 75% hexamethyldisilazane (HMDS) solution prepared in ethanol and finally in 100% HMDS. The probes were subjected to HMDS evaporation in a Euroclone AURA 2000 M.A.C. (BioAir, Sizzano, Pavia, Italy) fume hood. All samples were first air-dried and then metalized with a 100 Å thin silver layer, deposited using a BAL-TEC SCD 005 sputter coater (Schalksmühle, Germany). A FEI *Inspect S50* (Hillsboro, OR, USA) scanning electron microscope was used.

2.4.4. Statistical Analysis

All experiments were carried out in quadruplicates in order to achieve statistical significance. The statistical analysis was performed by using the unpaired Student's *t*-test and differences were considered significant for $p < 0.05$.

3. Results and Discussion

3.1. Cell Adhesion and Morphology

In vitro hMSC to OB phenotype differentiation is a long-lasting process (21 to 28 days), induced by specific osteogenic factors, which implies three cell stages: proliferation, differentiation, and maturation. Cell adhesion is an essential event that precedes the cell proliferation and differentiation. The process takes place before the formation of bone tissue and involves many proteins of the cytoskeleton that strongly interact with each other, such as integrins, actin filaments, and vinculin [35].

Cell adhesion is a parameter with a high specificity which characterizes relative sticking of the cell to a material or film. The evaluation of cell adhesion after longer incubation times provides relevant information regarding the behavior of cells on the surface of the biomaterials after implantation. In vivo, the biomaterial integration implies the formation of a stable interface between the extracellular matrix of the OB and the surface of the material. This excludes any intermediate fibrous tissue between the bone tissue and the surface of the material [36].

The hMSC and OB were grown onto the surface of Ti and BHA coatings for one and three days, and the samples were prepared for fluorescent microscopy imaging. The morphology and skeleton of the cells were investigated by labelling actin and vinculin, two proteins with important roles in the initiation of the cell adhesion process [37]. They are partially overlapping at the focal adhesion site, so the co-localization of the two proteins was investigated in all the tested samples.

After only one day in culture, in the presence of the OIM, the cells were already attached and presented an uniform pattern of spreading on the surface of both BHA and BHA:LiP coatings (Figure 1). After three days in culture, the cells revealed a pattern typical for actin (green) and vinculin (red) immunofluorescence labelling for all the tested samples. Thus, vinculin was easily spotted in focal contact sites, demonstrating the adhesion of the cells to the surface of the synthesized coatings, while the polymerized actin filaments network sustained the cells in this process. It is worth mentioning that the actin filaments form a dense cytoskeleton with a network-like appearance, indicating an optimum adhesion of the cells on the surface of the BHA and BHA:LiP coatings (Figure 1). Moreover, in the case of cells grown for three days onto the surface of the BHA:LiP coatings in the osteogenic medium, the actin filaments presented a circumferential pattern in the vicinity of the plasma membrane, while

the vinculin was present at focal contacts. All these features suggest an optimum adhesion of the cells promoting a good differentiation towards osteogenic fate (Figure 1). Indeed, in our previous study, the viability assays revealed that the presence of lithium as a doping reagent promoted the in vitro growth of the hMSC cells on the coating surface [23]. Moreover, it was demonstrated that the synthesized lithium-doped coatings exhibited low cytotoxicity and an excellent biocompatibility on human osteosarcoma MG63, new initiated dermal fibroblasts, and immortalized keratinocytes HaCaT cells [24]. Additionally, a long-lasting anti-staphylococcal and -fungal biofilm activity of the lithium-doped coatings was proved on the tested species, which are representative for the etiology of medical devices biofilm-associated infections [24].

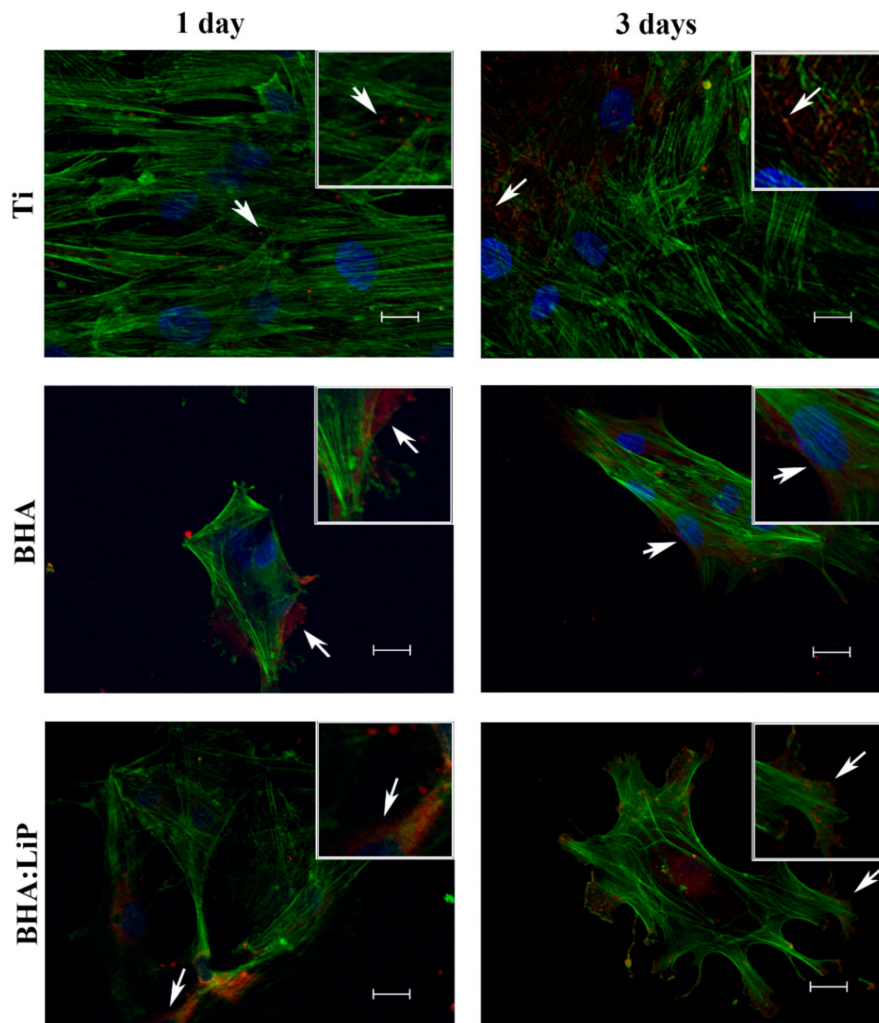


Figure 1. Cell morphology and cytoskeletal dynamic evaluation of human mesenchymal stem cells grown on the surface of Ti, biological-derived hydroxyapatite (BHA) and lithium-doped BHA (BHA:LiP) coatings after 1 and 3 days in culture. Green—actin; Red—vinculin; Blue—nucleus. Scale bar: 20 μm .

3.2. Analysis of ALP Activity

ALP is an enzyme present within all tissues of the body and is responsible for dephosphorization of a large number of molecules, such as deoxyribonucleic acid (DNA), ribonucleic acid (RNA), and some proteins under alkaline levels of pH inside the cell [38]. ALP concentration is higher in some organs such as liver, kidney, bone, placenta, and embryo or in the case of specific disease states [39,40]. All pluripotent cells, including embryonic stem cells or carcinoma embryonic cells, express ALP protein. However, during the differentiation process towards the osteoblastic phenotype, ALP expression in bone progenitor cells is enhanced, thus constituting an important early marker of

OB differentiation [34,41,42]. To further investigate the characteristics of the differentiation process of primary hMSC to OB grown on the surface of BHA and BHA:LiP coatings, the enzymatic activity of ALP inside the cells cultivated for 14 days was measured (Figure 2).

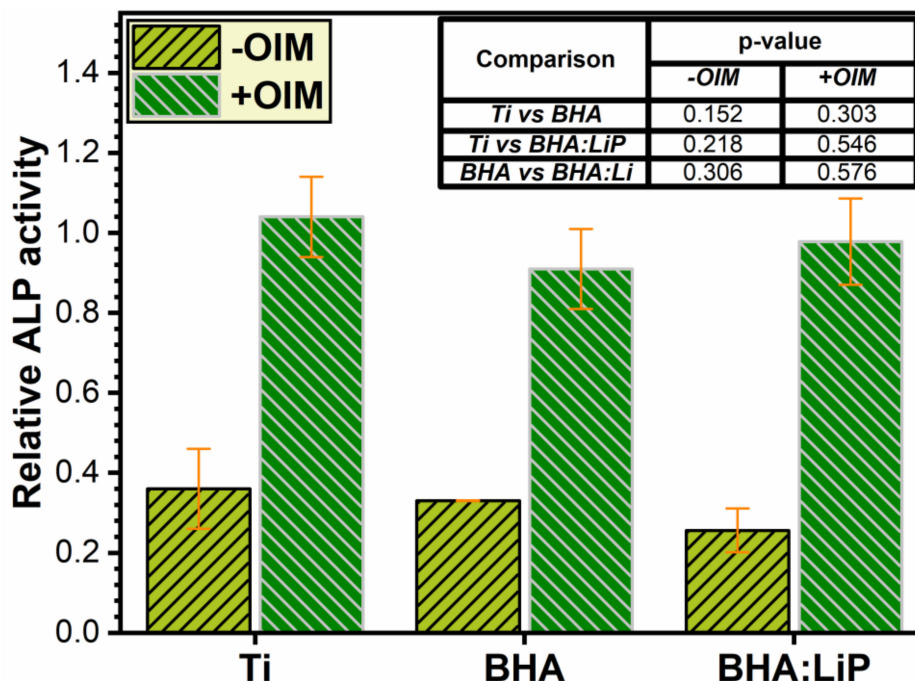


Figure 2. Alkaline phosphatase enzymatic activity detection in osteoblasts differentiated from primary human mesenchymal stem cells and grown on the surface of Ti, biological-derived hydroxyapatite (BHA) and lithium-doped BHA (BHA:LiP) coatings for 14 days, in the absence (–) or presence (+) of osteoinduction medium. Inset: table with the inferred p -values.

The in situ level of ALP, which is an early marker of osteogenic differentiation, in hMSC and differentiated OB after 14 days is depicted in Figure 2. The differences between the measured ALP levels were not found to be statistically significant for all the tested materials ($p > 0.05$ —inset to Figure 2). However, the value registered for the enzymatic activity in cells grown on all the tested surfaces (Ti, BHA and BHA:LiP coatings) is higher in the presence of osteoinduction medium (+OIM) than in its absence (–OIM) (Figure 2). In the case of BHA:LiP surface, the obtained results could be explained by the characteristics of the coatings induced by the lithium doping agent (low roughness values and a hydrophilic behavior) [23,24]. One should emphasize that all these enhanced properties of the BHA:LiP coatings could indicate their potential in better supporting the bone tissue formation.

3.3. Expression of OB-Specific Differentiation Markers

The OB cells have the ability to synthesize the major components of their matrix, such as collagenous and non-collagenous proteins, offering support for bone mineral deposition. The correct assembly of bone extracellular matrix assures mechanical stress resistance of bone tissue and constitutes a good basis for the successful osteogenesis and osteoinduction of an implant [43,44].

The cells' capacity to differentiate towards osteogenic phenotype was investigated by fluorescence microscopy and enzymatic assay using specific markers, i.e., osteocalcin and ALP. The expression of the osteocalcin marker in extracellular matrix was investigated in the presence or absence of OIM, after 21 days of cell differentiation on the surface of Ti, BHA, and BHA:LiP coatings.

As shown in Figure 3, in all tested samples, a low level of osteocalcin marker expression detected in hMSC after one day in culture could be observed. On the contrary, after 21 days in culture, the expression of osteocalcin can be observed in hMSC and is characterized by the presence of discrete

punctiform vesicles dispersed in a uniform manner throughout the cytoplasm. The pattern of dispersion of osteocalcin in the cell was observed for all tested materials and was previously reported by Sima et al. [32], in the case of OB cells cultivated on the surface of HA–sodium maleate–vinyl acetate copolymer coatings. These findings highlight a good biocompatibility of the BHA structures.

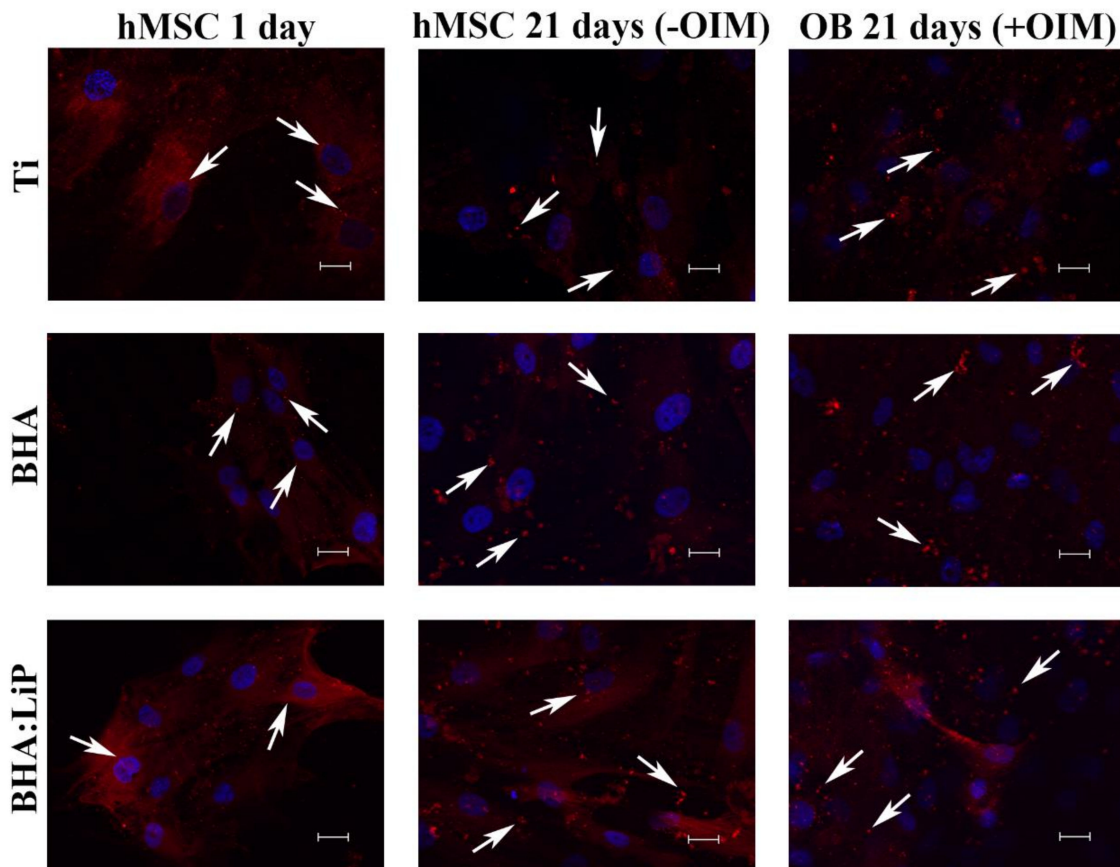


Figure 3. Investigation of osteocalcin expression in human mesenchymal stem cells and osteoblasts grown on the surface of Ti, biological-derived hydroxyapatite (BHA) and lithium-doped BHA (BHA:LiP) coatings after 1 and 21 days in culture. Red—osteocalcin; Blue—nucleus. Scale bar: 20 μm .

In the case of OB grown on the surface of BHA and BHA:LiP coatings, the presence of large granules was observed, in both the perinuclear region and near filamentous structures inside the cells. This pattern was more pronounced after 21 days of differentiation in the presence of OIM, suggesting that osteocalcin protein was engaged in the secretory pathway for the formation of extracellular matrix that surrounds the OB. Our results demonstrate that, in the presence of OIM, the cells grown on the surface of BHA and BHA:LiP coatings succeeded the differentiation towards osteoblastic phenotype.

3.4. Mineralization

As the cells differentiate from hMSC to OB, the expression of specific markers diminishes and the extracellular matrix mineralization process emerges. This specific morphological feature of calcium deposition and matrix mineralization characterizes the late stage of the osteogenesis process. Furthermore, the matrix mineralization was quantified by Alizarin Red dye detection (which specifically binds calcium ions) to evaluate the capacity of coatings to induce OB differentiation. The cells were grown for 28 days, in both the presence and absence of OIM.

As shown in Figure 4, the quantification of the bound dye revealed an enhanced secretion of calcium and thus a strong mineralization of the extracellular matrix by cells differentiated to OB and cultivated in OIM. One should note that the differences observed in the level of mineralization,

expressed by the values of Alizarin Red dye, were found to be statistically significant for all three analyzed situations. In addition, the level of mineralization in the case of BHA:LiP coatings was significantly higher as compared to control Ti.

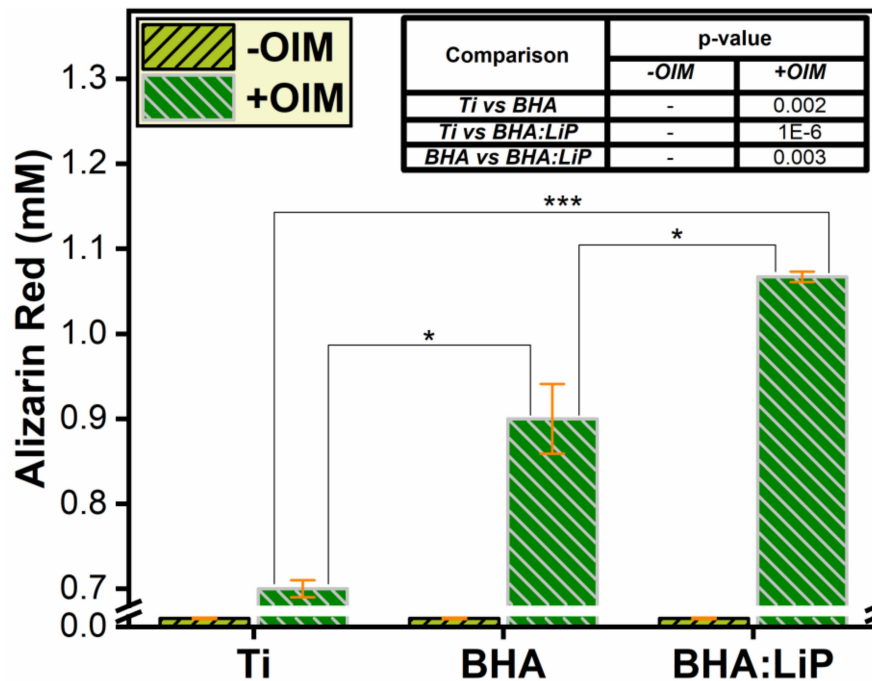


Figure 4. Extracellular matrix mineralization of osteoblasts differentiated from primary human mesenchymal stem cells grown on the surface of Ti, biological-derived hydroxyapatite (BHA), and lithium-doped BHA (BHA:LiP) coatings for 28 days, in the absence (–) or presence (+) of osteoinduction medium. Inset: table with the inferred *p*-values (* *p* < 0.05; *** *p* < 0.0001).

3.5. Structural Morphology of OB

The morphological investigation of attached cells offers important details on their interaction with the sample surfaces onto which they are grown. In this respect, SEM analysis was used to follow the dynamics of OB transformation from primary hMSC, over a period of 21 days. Moreover, the study of structural morphology details of OB helps build the picture of the progressive extracellular matrix mineralization and also elucidates the way the OB integrated in the mineralized matrix could maintain cellular connections with this natural biological support.

As shown in Figure 5, after 14 days in culture, the hMSC covered the surface of the materials, showing a good proliferation rate. Moreover, a typical fibroblast-like shape could be observed. In the case of cells grown in OIM, mineralization nodules were observed. However, a greater number of cells interconnected in the extracellular matrix was detected for BHA and BHA:LiP coatings. Visible differences could be observed between the morphology of cells grown on Ti and the ones cultivated on the surface of BHA and BHA:LiP coatings (Figure 5). Thus, in the latter case, the physical-chemical characteristics of the surface induced a proliferation in a tridimensional model.

The observed pattern was enhanced and could be easily observed after 21 days of differentiation on the surface of BHA and BHA:LiP coatings, in the presence of the OIM (Figure 6). The OB proliferated after three weeks in culture and secreted a mineralized extracellular matrix, the cells being inter-connected through dendritic processes and gap junctions, as previously described in literature [45–47]. This network of OB could constitute the premise for early differentiation of these cells grown onto the surfaces of BHA and BHA:LiP coatings *in vitro* and, consequently, for a better osteointegration *in vivo* [48,49]. This is in line with other studies showing that primary human osteoblastic cells were enabled to produce extracellular matrix and form an *ex vivo* 3D network

of osteocytes, which are the terminally differentiated bone cells, via biomimetic assembly using microfluidic perfusion culture [48]. Chen et al. [49] reported on mineralized matrix morphology in 3D culture of osteoblasts and revealed by SEM a synergistic cross-talk between 1α , $25(\text{OH})_2$ vitamin D3, and bone morphogenetic protein-2 that sustained improved osteogenesis and mineral deposition.

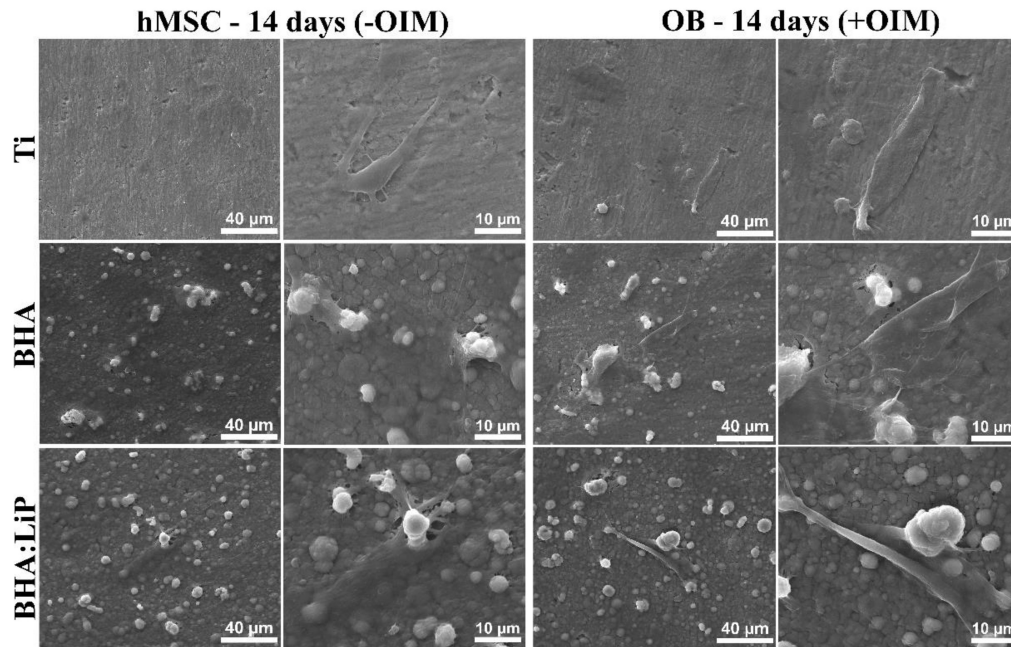


Figure 5. SEM micrographs of human mesenchymal stem cells differentiated to osteoblasts grown on the surface of Ti, biological-derived hydroxyapatite (BHA), and lithium-doped BHA (BHA:LiP) coatings for 14 days, in the absence or presence of osteogenic factors.

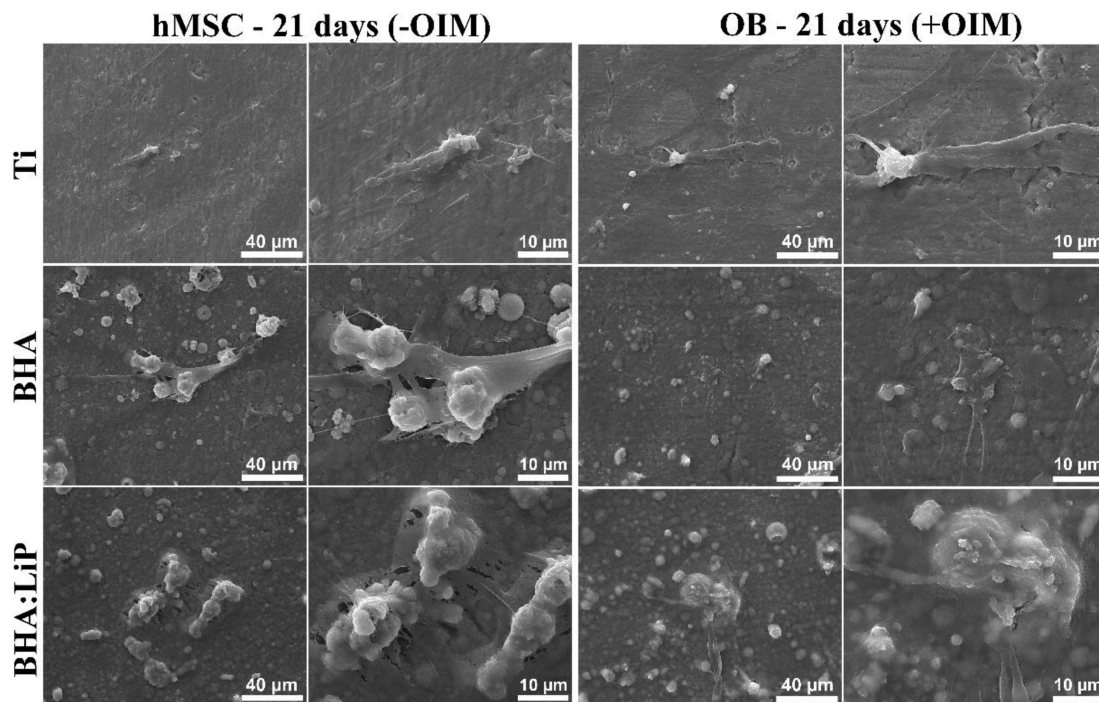


Figure 6. SEM micrographs of human mesenchymal stem cells differentiated to osteoblasts grown on the surface of Ti, biological-derived hydroxyapatite (BHA), and lithium-doped BHA (BHA:LiP) coatings for 21 days, in the absence or presence of osteogenic factors.

4. Conclusions

Biologically-derived hydroxyapatite (BHA) and lithium-doped BHA (BHA:LiP) coatings were synthesized by pulsed laser deposition onto medical-grade titanium (Ti) substrates. The morphological and cellular adhesion investigations performed in vitro showed that BHA:LiP coatings induced an enhanced adhesion of the primary human mesenchymal stem cells (hMSC) as compared to Ti or BHA coatings. The differentiation towards osteoblastic phenotype of hMSC grown on BHA and BHA:LiP coatings was demonstrated after cells cultured for a period of 21 days in osteogenic medium. In the case of cells grown on the surface of BHA:LiP coatings, large granules of osteocalcin protein were observed in the bone extracellular matrix, indicating a strong feature of the osteoblastic phenotype. In addition, the enzymatic activity of the alkaline phosphatase marker of osteogenic differentiation was increased in the case of cells grown on the surface of BHA:LiP coatings in the presence of osteogenic medium. In addition, the presence of numerous nodules of mineralization from osteoblast cells grown on the surface of BHA:LiP coatings, as well as a network-like organization of osteoblasts interconnected into the mineralized extracellular matrix, was evidenced. This network of osteoblasts could constitute the premise for early differentiation of cells grown on the surface of BHA:LiP coatings in vitro and, therefore, for an improved osteointegration in vivo.

Author Contributions: Conceptualization, P.E.F., L.D., and A.R.C.; Methodology, V.G.; Software, P.E.F., G.P.-P., and A.C.P.; Validation, P.E.F., L.D., F.N.O., R.W.E., and A.R.C.; Formal analysis, P.E.F., L.D., and A.R.C.; Investigation, G.P.-P. and P.E.F.; Resources, L.D., F.N.O., R.W.E., and A.R.C.; Data curation, P.E.F. and L.D.; Writing—original draft preparation, P.E.F., L.D., and A.R.C.; Writing—review and editing, P.E.F., L.D., V.G., G.P.-P., A.C.P., F.N.O., R.W.E., and A.R.C.; Visualization, P.E.F., L.D., V.G., G.P.P., A.C.P., R.W.E., and A.R.C.; Supervision, L.D.; Project administration, P.E.F., L.D., and A.R.C.; Funding acquisition, L.D. and A.R.C.

Funding: This work was supported by a grant from the Ministry of Research and Innovation, CNCS-UEFISCDI, No. PN-III-P1-1.1-PD-2016-1568 (PD 6/2018), within PNCDI III. L.D., A.P., V.G., and G.P.-P. acknowledge with thanks the partial support of the Romanian National Authority for Scientific Research and Innovation, CNCS-UEFISCDI, under Project No. PN-II-RU-TE-2014-1570 (TE 108/2015) and Core Programme—Contract 16N/2019. A.C.P. also acknowledges the support of CNCS-UEFISCDI in the framework of Contract PN-III-P1-1.1-TE-2016-2015 (TE136/2018). P.E.F. and A.R.C. acknowledge the support of the Institute of Biochemistry of the Romanian Academy under the Structural and Functional Proteomics Research Program.

Acknowledgments: All authors thank Livia Sima for useful discussions and for providing human mesenchymal stem cells for the experiments. All authors acknowledge George E. Stan for his useful comments and kind help.

Conflicts of Interest: The authors declare no conflict of interest.

References

1. Alvarez, K.; Nakajima, H. Metallic Scaffolds for Bone Regeneration. *Materials* **2009**, *2*, 790–832. [[CrossRef](#)]
2. Anselme, K. Biomaterials and interface with bone. *Osteoporos. Int.* **2011**, *22*, 2037–2042. [[CrossRef](#)] [[PubMed](#)]
3. Chen, S.; Guo, Y.; Liu, R.; Wu, S.; Fang, J.; Huang, B.; Li, Z.; Chen, Z.; Chen, Z. Tuning surface properties of bone biomaterials to manipulate osteoblastic cell adhesion and the signaling pathways for the enhancement of early osseointegration. *Colloids Surf. B Biointerfaces* **2018**, *164*, 58–69. [[CrossRef](#)]
4. Dohan Ehrenfest, D.M.; Coelho, P.G.; Kang, B.S.; Sul, Y.T.; Albrektsson, T. Classification of osseointegrated implant surfaces: Materials, chemistry and topography. *Trends Biotechnol.* **2010**, *28*, 198–206. [[CrossRef](#)] [[PubMed](#)]
5. Gaviria, L.; Salcido, J.P.; Guda, T.; Ong, J.L. Current trends in dental implants. *J. Korean Assoc. Oral Maxillofac. Surg.* **2014**, *40*, 50–60. [[CrossRef](#)]
6. Shah, F.A. Fluoride-containing bioactive glasses: Glass design, structure, bioactivity, cellular interactions, and recent developments. *Mater. Sci. Eng. C* **2016**, *58*, 1279–1289. [[CrossRef](#)]
7. Bouler, J.; Pilet, P.; Gauthier, O.; Verron, E. Biphasic calcium phosphate ceramics for bone reconstruction: A review of biological response. *Acta Biomater.* **2017**, *53*, 1–12. [[CrossRef](#)]
8. Narayanan, R.; Seshadri, S.K.; Kwon, T.Y.; Kim, K.H. Calcium phosphate-based coatings on titanium and its alloys. *J. Biomed. Mater. Res. Part B Appl. Biomater.* **2008**, *85*, 279–299. [[CrossRef](#)]
9. Yang, Y.; Dennison, D.; Ong, J.L. Protein adsorption and osteoblast precursor cell attachment to hydroxyapatite of different crystallinities. *Int. J. Oral Maxillofac. Implant* **2005**, *20*, 187–192.

10. Graziani, G.; Boi, M.; Bianchi, M. A Review on ionic substitutions in hydroxyapatite thin films: towards complete biomimetism. *Coatings* **2018**, *8*, 269. [CrossRef]
11. Vlădescu, A.; Pârâu, A.; Pană, I.; Cotruț, C.M.; Constantin, L.R.; Braic, V.; Vrânceanu, D.M. In vitro activity assays of sputtered HAp coatings with SiC addition in various simulated biological fluids. *Coatings* **2019**, *9*, 389. [CrossRef]
12. Jonauskas, V.; Stanionyte, S.; Chen, S.-W.; Zarkov, A.; Juskenas, R.; Selskis, A.; Matijosius, T.; Yang, T.C.K.; Ishikawa, K.; Ramanauskas, R.; et al. Characterization of sol-gel derived calcium hydroxyapatite coatings fabricated on patterned rough stainless steel surface. *Coatings* **2019**, *9*, 334. [CrossRef]
13. León, B.; Jansen, J.A. *Thin Calcium Phosphate Coatings for Medical Implants*; Springer: New York, NY, USA, 2009.
14. Batebi, K.; Khazaei, B.A.; Afshar, A. Characterization of sol-gel derived silver/fluor-hydroxyapatite composite coatings on titanium substrate. *Surf. Coat. Technol.* **2018**, *352*, 522–528. [CrossRef]
15. Roseti, L.; Parisi, V.; Petretta, M.; Cavallo, C.; Desando, G.; Bartolotti, I.; Grigolo, B. Scaffolds for Bone Tissue Engineering: State of the art and new perspectives. *Mater. Sci. Eng. C Mater. Biol. Appl.* **2017**, *78*, 1246–1262. [CrossRef] [PubMed]
16. Mariani, E.; Lisignoli, G.; Borzì, R.M.; Pulsatelli, L. Biomaterials: Foreign Bodies or Tuners for the Immune Response? *Int. J. Mol. Sci.* **2019**, *20*, 636. [CrossRef] [PubMed]
17. Chen, Z.; Klein, T.; Murray, R.Z.; Crawford, R.; Chang, J.; Wu, C.; Xiao, Y. Osteoimmunomodulation for the development of advanced bone biomaterials. *Mater. Today* **2016**, *19*, 304–321. [CrossRef]
18. Tite, T.; Popa, A.C.; Balescu, L.M.; Bogdan, I.M.; Pasuk, I.; Ferreira, J.M.F.; Stan, G.E. Cationic Substitutions in Hydroxyapatite: Current Status of the Derived Biofunctional Effects and Their In Vitro Interrogation Methods. *Materials* **2018**, *11*, 2081. [CrossRef]
19. Duta, L.; Popescu, A.C. Current Status on Pulsed Laser Deposition of Coatings from Animal-Origin Calcium Phosphate Sources. *Coatings* **2019**, *9*, 335. [CrossRef]
20. Chrisey, D.B.; Hubler, G.K. *Pulsed Laser Deposition of Thin Films*, 1st ed.; John Wiley & Sons: Hoboken, NJ, USA, 1994; pp. 1–649.
21. Eason, R. *Pulsed Laser Deposition of Thin Films—Applications—Led Growth of Functional Materials*; Wiley-Interscience: Hoboken, NJ, USA, 2006; pp. 1–682.
22. Christen, H.M.; Eres, G. Recent advances in pulsed-laser deposition of complex oxides. *J. Phys. Condens. Matter* **2008**, *20*, 264005. [CrossRef]
23. Popescu, A.C.; Florian, P.E.; Stan, G.E.; Popescu-Pelin, G.; Zgura, I.; Enculescu, M.; Oktar, F.N.; Trusca, R.; Sima, L.E.; Roseanu, A.; et al. Physical-chemical characterization and biological assessment of simple and lithium-doped biological-derived hydroxyapatite thin films for a new generation of metallic implants. *Appl. Surf. Sci.* **2018**, *439*, 724–735. [CrossRef]
24. Duta, L.; Chifiriuc, M.C.; Popescu-Pelin, G.; Bleotu, C.; (Pircalabioru) Gradisteanu, G.; Anastasescu, M.; Achim, A.; Popescu, A. Pulsed Laser Deposited Biocompatible Lithium-Doped Hydroxyapatite Coatings with Antimicrobial Activity. *Coatings* **2019**, *9*, 54. [CrossRef]
25. Vats, A.; Bielby, R.C.; Tolley, N.S.; Nerem, R.; Polak, J.M. Stem cells. *Lancet* **2005**, *366*, 592–602. [CrossRef]
26. Vohra, S.; Hennessy, K.M.; Sawyer, A.A.; Zhuo, Y.; Bellis, S.L. Comparison of mesenchymal stem cell and osteosarcoma cell adhesion to hydroxyapatite. *J. Mater. Sci. Mater. Med.* **2008**, *19*, 3567–3574. [CrossRef] [PubMed]
27. Duta, L.; Mihailescu, N.; Popescu, A.C.; Luculescu, C.R.; Mihailescu, I.N.; Cetin, G.; Gunduz, O.; Oktar, F.N.; Popa, A.C.; Kuncser, A.; et al. Comparative physical, chemical and biological assessment of simple and titanium-doped ovine dentine-derived hydroxyapatite coatings fabricated by pulsed laser deposition. *Appl. Surf. Sci.* **2017**, *413*, 129–139. [CrossRef]
28. Duta, L.; Oktar, F.N.; Stan, G.E.; Popescu-Pelin, G.; Serban, N.; Luculescu, C.; Mihailescu, I.N. Novel doped hydroxyapatite thin films obtained by pulsed laser deposition. *Appl. Surf. Sci.* **2013**, *265*, 41–49. [CrossRef]
29. Eisenhart, S. EU Regulation 722. In *New EU Animal Tissue Regulations in Effect for Some Medical Devices*; Emergo: Hong Kong, China, 2013; Available online: <https://www.emergobyul.com/blog/2013/09/new-eu-animal-tissue-regulations-effect-some-medical-devices> (accessed on 29 August 2019).
30. ISO 22442-1. *Medical Devices Utilizing Animal Tissues and Their Derivatives—Part 1: Application of Risk Management*; International Organization for Standardization: Berlin, Germany, 2015.
31. Negroiu, G.; Piticescu, R.M.; Chitanu, G.C.; Mihailescu, I.N.; Zdrentu, L.; Miroiu, M. Biocompatibility evaluation of a novel hydroxyapatite-polymer coating for medical implants (in vitro tests). *J. Mater. Sci.* **2008**, *19*, 1537–1544. [CrossRef]

32. Sima, L.E.; Filimon, A.; Piticescu, R.M.; Chitanu, G.C.; Suflet, D.M.; Miroiu, M.; Socol, G.; Mihailescu, I.N.; Neamtu, J.; Negroiu, G. Specific biofunctional performances of the hydroxyapatite–sodium maleate copolymer hybrid coating nanostructures evaluated by in vitro studies. *J. Mater. Sci. Mater. Med.* **2009**, *20*, 2305–2316. [[CrossRef](#)]
33. Gregory, C.A.; Gunn, W.G.; Peister, A.; Prockop, D.J. An Alizarin red-based assay of mineralization by adherent cells in culture: Comparison with cetylpyridinium chloride extraction. *Anal. Biochem.* **2004**, *329*, 77–84. [[CrossRef](#)]
34. Sima, L.E.; Stan, G.E.; Morosanu, C.O.; Melinescu, A.; Ianculescu, A.; Melinte, R.; Neamtu, J.; Petrescu, S.M. Differentiation of mesenchymal stem cells onto highly adherent radio frequency-sputtered carbonated hydroxylapatite thin films. *J. Biomed. Mater. Res. A* **2010**, *95*, 1203–1214. [[CrossRef](#)]
35. Brakebusch, C.; Fassler, R. The integrin-actin connection, an eternal love affair. *EMBO J.* **2003**, *22*, 2324–2333. [[CrossRef](#)]
36. Anselme, K. Osteoblast adhesion on biomaterials. *Biomaterials* **2000**, *21*, 667–681. [[CrossRef](#)]
37. Okumura, A.; Goto, M.; Goto, T.; Yoshinari, M.; Masuko, S.; Katsuki, T.; Tanaka, T. Substrate affects the initial attachment and subsequent behavior of human osteoblastic cells (Saos-2). *Biomaterials* **2001**, *22*, 2263–2271. [[CrossRef](#)]
38. Hoylaerts, M.F.; Manes, T.; Millan, J.L. Mammalian alkaline phosphatases are allosteric enzymes. *J. Biol. Chem.* **1997**, *272*, 22781–22787. [[CrossRef](#)] [[PubMed](#)]
39. Sharma, U.; Pal, D.; Prasad, R. Alkaline phosphatase: An overview. *Indian J. Clin. Biochem.* **2014**, *29*, 269–278. [[CrossRef](#)]
40. Weiss, M.J.; Henthorn, P.S.; Lafferty, M.A.; Slaughter, C.; Raducha, M.; Harris, H. Isolation and characterization of a cDNA encoding a human liver/bone/kidney-type alkaline phosphatase. *Proc. Natl. Acad. Sci. USA* **1986**, *83*, 7182–7186. [[CrossRef](#)]
41. Gronthos, S.; Zannettino, A.C.; Graves, S.E.; Ohta, S.; Hay, S.J.; Simmons, P.J. Differential cell surface expression of the STRO-1 and alkaline phosphatase antigens on discrete developmental stages in primary cultures of human bone cells. *J. Bone Miner. Res.* **1999**, *14*, 47–56. [[CrossRef](#)]
42. Dos Santos, E.A.; Farina, M.; Soares, G.A.; Anselme, K. Chemical and topographical influence of hydroxyapatite and beta-tricalcium phosphate surfaces on human osteoblastic cell behavior. *J. Biomed. Mater. Res. A* **2009**, *89*, 510–520. [[CrossRef](#)]
43. Hamilton, D.W.; Chehroudi, B.; Brunette, D.M. Comparative response of epithelial cells and osteoblasts to microfabricated tapered pit topographies in vitro and in vivo. *Biomaterials* **2007**, *28*, 2281–2293. [[CrossRef](#)]
44. Kunzler, T.P.; Drobek, T.; Schuler, M.; Spencer, N.D. Systematic study of osteoblast and fibroblast response to roughness by means of surface-morphology gradients. *Biomaterials* **2007**, *28*, 2175–2182. [[CrossRef](#)]
45. Van de Peppel, J.; van Leeuwen, J.P.T.M. Vitamin D and gene networks in human osteoblasts. *Front. Physiol.* **2014**, *5*, 137. [[CrossRef](#)]
46. Dallas, S.L.; Prideaux, M.; Bonewald, L.F. The osteocyte: An endocrine cell... and more. *Endocr. Rev.* **2013**, *34*, 658–690. [[CrossRef](#)] [[PubMed](#)]
47. Popescu, A.C.; Sima, F.; Duta, L.; Popescu, C.; Mihailescu, I.N.; Capitanu, D.; Mustata, R.; Sima, L.E.; Petrescu, S.M.; Janackovic, D. Biocompatible and bioactive nanostructured glass coatings synthesized by pulsed laser deposition: In vitro biological tests. *Appl. Surf. Sci.* **2009**, *255*, 5486–5490. [[CrossRef](#)]
48. Sun, Q.; Choudhary, S.; Mannion, C.; Kissin, Y.; Zilberberg, J.; Lee, W.Y. Ex vivo construction of human primary 3D-networked osteocytes. *Bone* **2017**, *105*, 245–252. [[CrossRef](#)] [[PubMed](#)]
49. Chen, J.; Dosier, C.R.; Park, J.H.; De, S.; Guldberg, R.E.; Boyan, B.D.; Schwartz, Z. Mineralization of three-dimensional osteoblast cultures is enhanced by the interaction of 1 α ,25-dihydroxyvitamin D3 and BMP2 via two specific vitamin D receptors. *J. Tissue Eng. Regen. Med.* **2016**, *10*, 40–51. [[CrossRef](#)]

